#10 518

Investigation of Atrium Smoke Exhaust Effectiveness

Gary D. Lougheed, Ph.D.
Member ASHRAE

George V. Hadjisophocleous, Ph.D., P.Eng.

ABSTRACT

This paper presents results of a project initiated by ASHRAE and the National Research Council of Canada. The project applies both physical and numerical modeling techniques to atrium smoke exhaust systems to investigate the effectiveness of such systems and to develop guidelines for their design.

This paper compares experimental results obtained from testing a physical model of a mechanically exhausted atrium space with results of two sets of numerical predictions of the same space. One set of numerical predictions uses standard plume equations; the other set uses computational fluid dynamics (CFD). This paper also investigates the effect of fire size and opening location on the conditions in the atrium.

INTRODUCTION

An atrium within a building is a large open space created by an opening or series of openings in floor assemblies, thus connecting two or more stories of a building.[1] This design feature has gained considerable popularity, mainly because of its visual appeal. The sides of an atrium may be open to all floors, to some of the floors, or closed to all or some of the floors by unrated or rated fire-resistant construction. As well, there may be two or more atria within a single building, all interconnected at the ground floor or on a number of floors.

By interconnecting floor spaces, an atrium violates the concept of floor-to-floor compartmentation, which is intended to limit the spread of fire and smoke from the floor of fire origin to other stories inside a building. With a fire on the floor of an atrium or in any space open to it, smoke can fill the atrium and connected floor spaces. Elevators, open stairs, and egress routes that are within the atrium space can also become smoke-laden.

Protecting the occupants of a building from the adverse effects of smoke in the event of a fire is one of the primary objectives of any fire protection system design. Achieving this objective becomes more difficult when dealing with large spaces such as an atrium or an indoor sports arena, where a large number of occupants may be present and the compartment geometries may be complex. Because of these difficulties, model building codes place restrictions on the use of atrium spaces in buildings. Some of the requirements that are commonly applied in codes for buildings with atria include

- the installation of automatic sprinklers throughout the building,
- limits on combustible materials on the floor of an atrium,
- the installation of mechanical exhaust systems for use by firefighters, and
- the provision of smoke management systems to maintain tenable conditions in egress routes.

Atrium smoke management systems have become common in recent years, and design information for these systems is provided in NFPA 92B (1995) and Klote and Milke (1992). There are, however, a number of situations that may detrimentally impact the effectiveness of the smoke management system. These include obstructions in the smoke plume (Hansell and Morgan 1994) or the formation of a prestratification layer in the atrium (Klote 1994). In the former case, smoke may be directed to adjacent spaces or mixed with the air within the zone in which tenable conditions are required. In the latter case, the smoke produced by the fire may not reach the

1. For the purposes of this paper, the definition of "atrium" will be in accordance with that used in NFPA 92B (1995) and by Klote and Milke (1992), that is, a large-volume space in a commercial building. This includes office buildings, hotels and hospitals with typical atrium spaces, covered malls, and other buildings with similar large-volume spaces. It does not include warehouses, manufacturing facilities, or other similar spaces with high fire load densities.

Gary D. Lougheed and **George V. Hadjisophocleous** are senior research officers at the National Fire Laboratory, Institute for Research in Construction, National Research Council Canada, Ottawa, Ont.

ceiling, where it could be exhausted. Also, in this case, smoke buildup could occur at a height at which it can migrate into the communicating spaces.

Under some conditions, another phenomenon may impact the effectiveness of a smoke management system: air from the lower (cold) layer can mix with the smoke in the upper layer as it is being exhausted by the smoke management system. This phenomenon reduces the effectiveness of the smoke management system (Hinckley 1995). As a result, the clear height in the atrium is reduced and people in some spaces may be exposed to smoke and toxic fire gases. This phenomenon is referred to as "plugholing" and investigations on this have been carried out using natural venting systems (Morgan and Gardiner 1990; Spratt and Heselden 1974). To study the effects of plugholing on a mechanical exhaust system used for atrium smoke management, a joint research project was initiated by ASHRAE and the National Research Council of Canada in 1995. This project includes both physical and numerical modeling of an atrium smoke management system. The objective of the project is to develop methods with which designers can account for the mixing of cold air with the smoke exhaust. These methods will provide a basis for the design of cost-effective smoke management systems that will meet design expectations.

This paper presents the initial results of physical model studies of an atrium space with mechanical exhaust. It includes a comparison between experimental data and computational fluid dynamics (CFD) model predictions of the conditions in the atrium space. It also investigates the effect of fire size and opening location on the conditions in the atrium.

ATRIUM SMOKE MANAGEMENT

Smoke management systems are defined as engineered systems that include all methods that can be used singly or in combination to reduce smoke production or to modify smoke movement. The objectives of a smoke management system are to reduce deaths and injuries from smoke, reduce property loss from smoke damage, and to aid firefighters (Klote and Milke 1992). In this section, the methods used for atrium smoke management applications are reviewed.

Methods to reduce smoke production in atria include the installation of automatic sprinklers and limitations on the quantity of combustible materials used in the construction of the building and located on the floor of the atrium. Sprinklers are effective in suppressing[2] fires in floor spaces with limited ceiling heights, but, because of delayed response, sprinklers may not be effective in suppressing fires in spaces with ceiling heights greater than 11 to 15 m (36 to 49.2 ft) (Degenkolb 1975, 1983) or in controlling[3] fires in atria exceeding 20 m (65.6 ft) in height (Tamura 1995). Engineering guides such as NFPA 92B (1995) generally assume that, unless there is information to indicate otherwise, the effect of sprinklers on the design fire size can be accounted for by assuming that the fire stops growing when sprinklers are actuated. The fire continues to burn at this size until the involved fuel is consumed (NFPA 1995).

Because of these limitations on sprinklers in high spaces, some building codes, such as the National Building Code of Canada (NBCC 1995), place limits on the quantity of combustible materials located on the floor of an atrium. Based on the NBCC, the combustible content in an atrium space is limited to 16 g/m^3 (0.001 lb/ft^3) of volume in the interconnected space in which the ceiling height is greater than 8 m (26.2 ft). However, as noted by Tamura (1995), even with efforts to limit smoke production by limiting the quantity of combustibles in the atrium, smoke logging of an atrium can still occur. This is particularly true for small atria, where there is a minimum volume for storing the smoke. Furthermore, it is difficult to control the quantity of combustibles in an atrium with many changes occurring in the contents from week to week over the lifetime of a building. Transient fuels that can be in an atrium include packing materials, Christmas decorations, displays, construction materials, and furniture being moved to another part of the building (Klote 1994).

Klote and Milke (1992) recommend design fires of approximately 2,000 kW and 5,000 kW for atria with restricted fuel and atria with combustibles, respectively. These design fires are similar to those required in the BOCA (1996) and UBC (ICBO 1994) building codes and are used as the basis for the studies discussed in this paper.

Passive methods to modify smoke movement include the use of smoke barriers or draft curtains to limit smoke incursion into communicating spaces and egress routes. Another passive method is to allow the smoke to fill the upper portion of the atrium space while the occupants evacuate the atrium. The latter approach applies only to large-volume spaces where the smoke-filling time is sufficient for both occupant response and evacuation (Klote 1994).

For those cases in which passive smoke management methods produce insufficient time for occupant response and evacuation, upper layer mechanical exhaust systems are frequently used to maintain the smoke level above the occupants until they are able to evacuate. This active system decreases the rate at which the smoke layer descends in the atrium. Tests conducted by Yamana and Tanaka (1985) demonstrated that such a system could be effective for smoke management purposes. However,

2. NFPA 13 (1996) defines fire suppression as sharply reducing the heat release rate of a fire and preventing its regrowth by means of direct and sufficient application of water through the fire plume to the burning fuel surface.

3. NFPA 13 (1996) defines fire control as limiting the size of a fire by distribution of water so as to decrease the heat release rate and pre-wet adjacent combustibles while controlling ceiling gas temperatures to avoid structural damage. This is the generally acceptable level of performance for an automatic sprinkler system in codes and standards.

since the rate at which smoke descends in the atrium is dependent on the heat release rate of the fire and on the height of the smoke layer, the design of an active system requires the use of a numerical fire model (Klote 1994).

A common approach for the design of an upper layer mechanical exhaust system for atrium smoke management is to design a system that will maintain the smoke at a steady clear height assuming a steady-state design fire. Such a system can be designed using a calculation method based on plume equations. This method is included in the BOCA (1996) and UBC (ICBO 1994) building codes for use in those cases in which basic methods (i.e., passive systems) are unable to meet the design requirements. This is the method investigated in the physical and CFD modeling studies discussed in this paper.

DESCRIPTION OF PHYSICAL MODEL

Test Facility

The experimental facility used for this study is shown in Figure 1. The facility is a large compartment with dimensions of 9 m by 6 m by 5.5 m (29.5 ft by 19.7 ft by 18 ft) with a door on the west wall near the southwest corner and a door on the east wall near the northeast corner. The interior wall surface of the compartment was insulated using 25 mm (0.9 in.) thick rock fiber insulation that was used for two reasons: to protect the walls of the facility so that high gas temperatures could be attained during the tests and to provide a better boundary condition for the CFD runs.

A fan was used to supply fresh air into the compartment through openings in the floor around the walls, as shown in Figure 1. The openings were designed to maintain the velocity of the incoming air to less than 1 m/s (3.2 ft/s) for the maximum airflow expected, which was between 2 and 4 m^3/s. These openings had a width of 0.1 m (0.3 ft) and a total length of 22.8 m (74.8 ft). The inlet air was supplied to the four sides of the room through a duct system in the underfloor space. It was balanced using dampers in the four supply branches.

Thirty-two exhaust inlets with a diameter of 150 mm (5.9 in.) were located in the ceiling of the compartment, as shown in Figure 1. These inlets were used to extract the hot gases from the compartment during the tests. All exhaust ducts were connected to a central plenum. A 0.6 m (1.9 ft) diameter duct was used between the plenum and an exhaust fan. By using multiple exhaust inlets, smoke exhaust system parameters such as total area of exhaust inlet, velocity at the inlets, and exhaust inlet location relative to the ceiling and the fire could be readily investigated.

The exhaust system included a two-speed fan with nominal capacities of 3 and 4 m^3/s. The actual volumetric flow rate produced by the fan in a test depended on a number of factors, including smoke temperature and the number of exhaust inlets used. Therefore, the volumetric flow rate in the main duct was continuously measured throughout a test.

A square propane sand burner was used for the fire source. The burner was capable of simulating fires ranging from 15 kW to 1,000 kW with three possible fire areas: 0.145 m^2 (1.56 ft^2), 0.58 m^2 (6.2 ft^2), and 2.32 m^2 (24.9 ft^2). The heat release rate of the fire was determined using two methods. The first method computes the heat release rate from the volume flow rate of propane supplied to the burner. The second method was based on the oxygen depletion method using oxygen concentrations, temperature, and volume flow rate measured in the main exhaust duct.

With the small heat releases and large volumetric flow rates used for a number of tests, the depletion of oxygen in the exhaust gases was at or below the level for accurate heat release rate measurements using the oxygen depletion method. For these cases, the heat release rate was determined using the measured flow rate of propane into the burner. The oxygen depletion method was used to verify the heat release rate results for the larger fires.

Instrumentation

The room was instrumented with thermocouples and pitot tubes for velocity measurements. Also, gas inlets were located in the room for extracting gas samples to determine CO_2 concentrations at various locations. The locations of the instrumentation are shown in Figure 1.

Twelve CO_2 inlets were located at the southwest quarter point at various heights, as shown in Figure 1. The CO_2 inlets were connected to two CO_2 analyzers. A solenoid valve system was used to switch between the sampling points during a test. For each point, the analyzers were purged for 30 seconds before a measurement was made. Six additional CO_2 inlets were located in pairs at the northwest, southeast, and southwest quarter points of the room at the same levels as CO_2 inlets 8 and 11 shown in Figure 1.

A set of 19 thermocouples was located at the center of the room over the propane burner, as shown in Figure 1 (section B-B). Eight thermocouples were located along the vertical centerline, six thermocouples were located at 250-mm (9.8-in.) intervals along a horizontal line at a height of 3 m (9.8 ft), and another five thermocouples were located at 250-mm (9.8-in.) intervals along a horizontal line at a height of 4.5 m (14.7 ft). Four additional thermocouples were located along a horizontal line near the ceiling at 1-m (3.2 ft) intervals.

A second set of thermocouples was located below the southwest duct inlet as shown in Figure 1 (section A-A). These thermocouples were used to measure the gas temperatures around the exhaust inlets to determine whether fresh air was exhausted from the room. A thermocouple tree was located at the southwest quarter point with 15 thermocouples. These thermocouples, together with the CO_2 measurements at the same locations, were used to determine the depth of the hot layer in the room.

Velocity measurements using pitot tubes were taken at the northwest exhaust inlet. One velocity probe was located inside the exhaust duct. Two probes were located below the port at distances of 250 mm (9.8 in.) and 500 mm (19.6 in.). A bidirectional probe was located 250 mm (9.8 in.) below the duct inlet and 75 mm (2.9 in.) from its center to measure horizontal veloc-

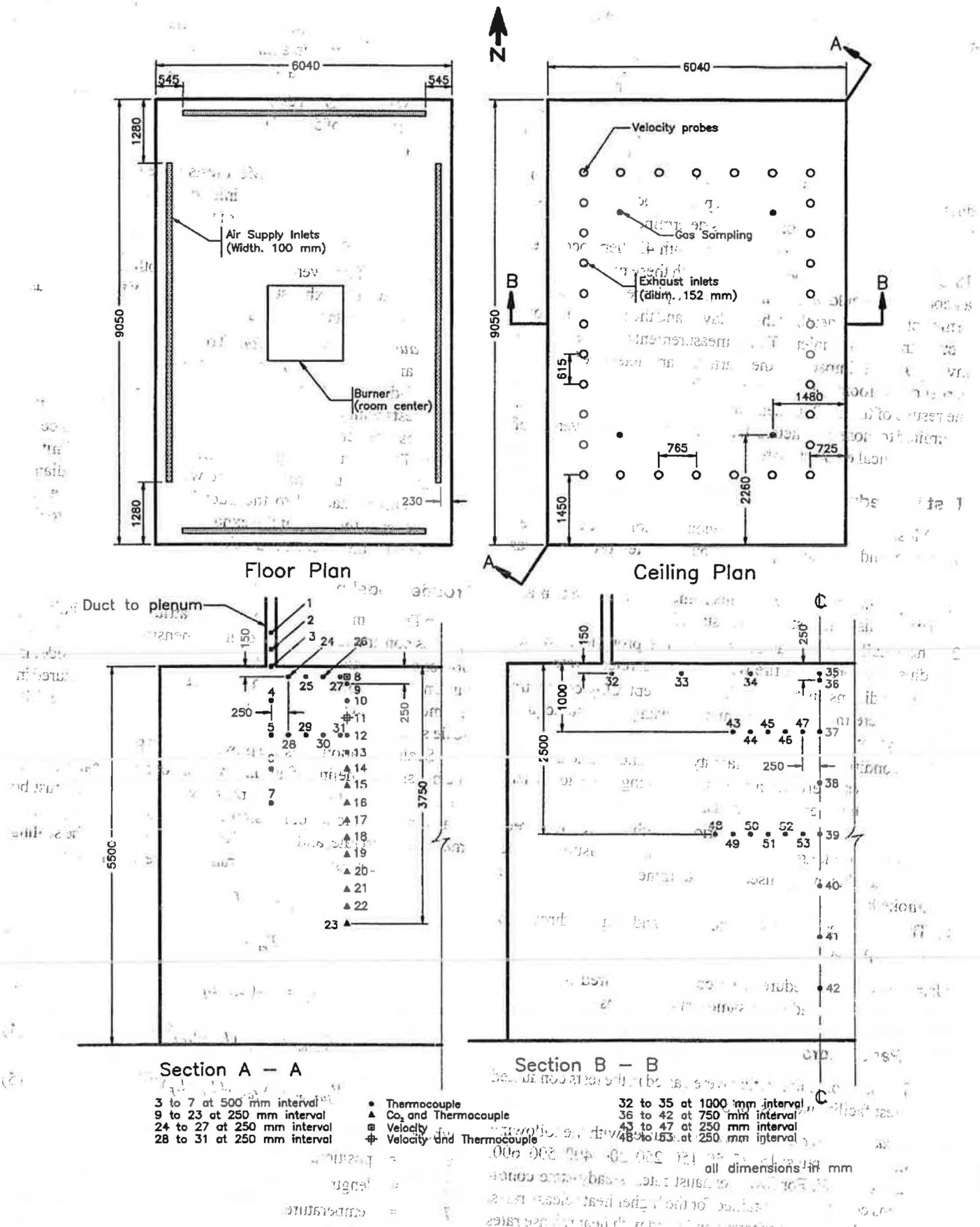

Figure 1 *Room dimensions and instrumentation.*

ities. These velocity measurements were used to determine the flow conditions around an exhaust inlet.

The volume flow rate, temperature, CO, CO_2, and oxygen concentrations were measured in the main exhaust duct. These measurements were used to determine the heat release rate of the fire, as well as to calculate the exhaust rate of the ventilation system. A pitot tube and thermocouple, located at the center of the duct, were used to determine the volumetric flow rate in the duct. A pitot traverse was conducted prior to the test program. A shape factor for the duct of 0.91 was determined.

In all, the room was instrumented with 43 thermocouples, 18 CO_2 inlets, and 4 velocity probes. With these measurements, a good picture could be obtained of the fire plume, the conditions in the hot layer, the depth of the hot layer, and the flow conditions around the exhaust inlets. These measurements can be used to investigate the impact of the various parameters referred to earlier on the room conditions and to allow for comparisons with the results of the CFD model. For this paper, the discussion will be limited to those parameters that determine the effectiveness of the mechanical exhaust system.

Test Procedure

Most tests described in the previous section were conducted over an extended period (up to one hour). The test procedure was as follows.

1. All systems, including the mechanical exhaust system and data acquisition system, were started.
2. The small burner was ignited and the propane flow rate adjusted to provide a fire with a low heat release rate.
3. All conditions in the test facility, except CO_2 concentrations, were monitored continuously using the data-acquisition system.
4. The conditions in the test facility were allowed to stabilize for approximately 15 minutes, producing a steady, clear height with upper layer exhaust.
5. The CO_2 concentrations at various heights were measured. These data, along with the temperatures measured at the same heights, were used to determine the height of the smoke layer.
6. The heat release rate was increased and steps 3 through 5 were repeated.

Using this test procedure, data could be acquired for several heat release rates under the same test conditions.

Test Parameters

The main parameters that were varied in the tests conducted in the test facility were as follows.

1. *Heat release rate.* Tests were conducted with the following heat release rates: 15, 25, 50, 150, 250, 300, 400, 500, 600, and 800 kW. For lower exhaust rates, steady-state conditions could not be obtained for the higher heat release rates. Thus, the number of tests conducted with heat release rates greater than 500 kW was limited.
2. *Number of exhaust inlets.* Tests were conducted with 1, 4, 16, and 32 exhaust inlets with the exhaust inlets 150 mm (5.9 in.) in diameter. In addition, tests were conducted with 32 exhaust inlets with a 75 mm (2.9 in.) diameter.
3. *Exhaust inlet height.* Tests were conducted with the exhaust inlets at heights of 5.5 m (18 ft), 150 mm below the ceiling, 4.5 m (14.7 ft), and 3.5 m (11.4 ft).
4. *Exhaust inlet orientation.* Most tests were conducted with the centerline of the exhaust inlet oriented vertically. For comparison, a limited number of tests were conducted with the centerline of the exhaust inlets oriented horizontally.
5. *Fan speed.* Tests were conducted with both fan speeds for the tests with 32 exhaust inlets. Only the low fan speed was used for the tests with 4 and 16 exhaust inlets.
6. *Exhaust inlet configuration.* To allow flexibility in the test arrangement, most tests were conducted with the small-diameter duct projecting into the test facility. Only the tests with the exhaust inlet at the 5.5-m (18-ft) height represented conditions with the exhaust inlet near a ceiling. To further investigate the effect of a ceiling, a limited number of tests were conducted with a 1 m (3.2 ft) diameter collar attached to the duct just above the inlet. In these tests, the flow at the exhaust inlet was similar to the case with the inlet near a ceiling.

Froude Modeling

In Froude modeling, a model of an atrium or other building space is constructed such that every dimension is an exact fraction of a full-scale facility. Tests are conducted in the model in air at normal atmospheric conditions. Temperatures measured in the model are the same as the corresponding places in the full-scale system.

Scaling relationships are provided in NFPA 92B (1995) for the physical modeling of atrium spaces. For a physical model of an atrium exhaust system, the primary parameters that must be scaled are the model dimensions, temperature, velocity, volumetric exhaust rate, and convective heat release rate. The scaling expressions for each of these parameters are as follows:

$$x_m = x_F(L_m/L_F) \tag{1}$$

$$T_m = T_F \tag{2}$$

$$v_m = v_F(L_m/L_F)^{1/2} \tag{3}$$

$$Q_{c,m} = Q_{c,F}(L_m/L_F)^{5/2} \tag{4}$$

$$V_{fan,m} = V_{fan,F}(L_m/L_F)^{5/2} \tag{5}$$

where

x = position,
L = length,
T = temperature,
v = velocity,

Q_c = convective heat release rate,
V_{fan} = volumetric exhaust rate,
F = full-scale, and
m = reduced-scale model.

For the range of heat release rates used in the test facility (15 kW to 800 kW) and using Equation 4, the physical model tests provide physical scalings ranging from approximately one-half to one-tenth for a 5,000-kW steady-state design fire. The tests thus simulate atria with heights ranging from approximately 11 m to 55 m (36 to 180.4 ft). However, as is noted in NFPA 92B (1995) and by Klote (1994), physical scaling greater than one-eighth should be applied with considerable caution. For a 2,000-kW design fire, the tests provide physical scaling in the range of approximately one-half to one-eighth.

A second test facility with all dimensions approximately two times the test facility described above is under preparation. Selected tests will be conducted with this facility to simulate test conditions in the small-scale test arrangement. In addition, this test facility will be used to extend the physical modeling to higher atria (up to approximately 100 m [328 ft]).

In this paper, the results of the physical model described previously are compared to those obtained using the engineering equations provided in NFPA 92B (1995) and to the CFD model. These comparisons are used to verify the models as the basis for determining the parameters that affect mechanical exhaust effectiveness in an atrium.

DESCRIPTION OF NUMERICAL (CFD) MODEL

For numerical modeling, this project used a general three-dimensional computational fluid dynamics model with capabilities in handling laminar and turbulent flows, incompressible and compressible multicomponent fluids, porous media, Lagrangian particle tracking, reacting combusting flows, conjugate heat transfer, surface-to-surface radiation, rotating frames of reference, and subsonic, transonic, and supersonic flows (ASC 1994). The grid generation features of the model include the ability to handle nonorthogonal boundary fitted grids, grid embedding, and grid attaching.

The fire was modeled using a flamelet model (Peters 1984, 1986). In this model, only two user-defined scalar equations are used: one is the mixture fraction and the other is the variance of the mixture fraction. In this simulation, propane was used as fuel and the following 12 chemical species were used from the model's libraries: C_3H_8, O_2, H, O, H_2, H_2O, CO, CO_2, CH_3, CH_4, C_2H_2, and C_2H_4.

Turbulent flow was specified using the k-ε model, and all turbulent walls used the log-law treatment. The walls of the room were all treated as adiabatic. The boundaries at the outflow openings were defined as mass flow boundaries with a total mass flow rate corresponding to the flow rate used in the experiments. The experimental propane mass flow rate was defined at the fire surface. All fresh air inlets were defined using a constant static pressure.

Radiation exchange between the hot gases and the surroundings was modeled using the diffusion radiation model (ASC 1994) with a gas absorption coefficient of 0.15.

One-fourth of the test room described previously was chosen as the computational domain due to the symmetric flow characteristics observed in both the experimental tests and preliminary model simulations. The whole computational domain was divided into a grid of 21 by 31 by 21 control volumes. Additional grid points were embedded around the fire source and the exhaust inlets to enable better resolution of the solution in these areas. To simulate the small-scale test facility, the total number of grid points for the simulation was 22,496.

EXPERIMENTAL RESULTS

Steady-State Test Conditions

As noted in the test procedure, the propane flow rate was adjusted to a predetermined level to produce the required heat release rate. Figure 2 shows a test with a total heat release rate of approximately 25 kW in the initial stage and 250 kW in the later stage of the test. The fire was maintained steady for up to 15 minutes at each heat release rate to allow stable conditions to be reached in the test facility.

The temperature profiles measured at various heights in the test facility are given in Figure 3 for the heat release rates shown in Figure 2. For the case of the low heat release rate, the temperature profile in the hot layer quickly stabilized to a relatively steady condition. For the higher heat release cases (> 200 kW), the radiation from the fire produces some heating of the walls and air in the lower levels of the test facility. As a result, the temperature profiles in the upper layer did not reach a steady condition. However, in the later stages of the test, the

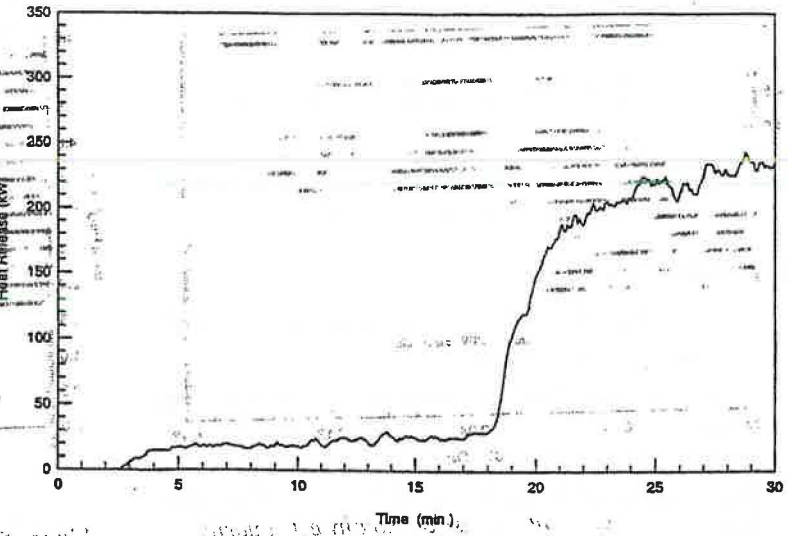

Figure 2 Heat release rate.

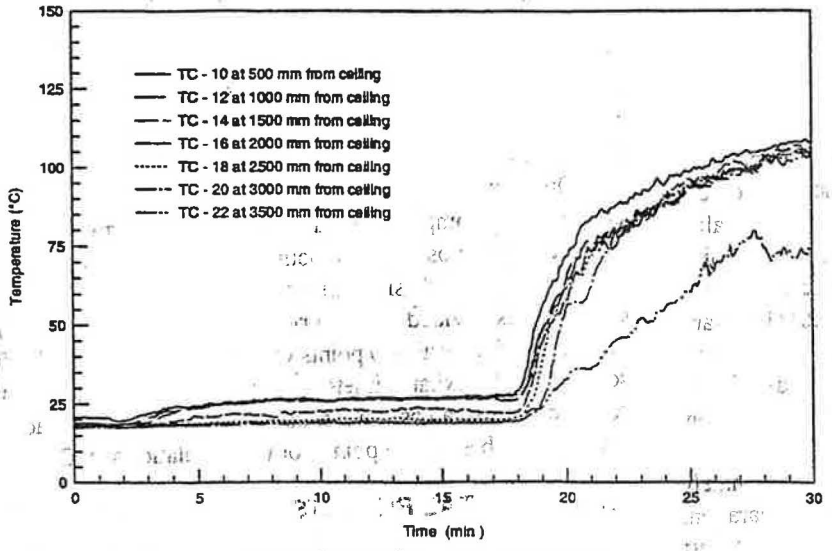

Figure 3 Temperature at the southwest quarter point.

temperature increase was minimal and is assumed to be approximately steady.

Smoke Interface

Once the conditions in the test facility stabilized, the CO_2 concentrations were measured at several heights in the test facility at the southwest quarter point of the test facility (Figure 1). Using the temperature profiles measured during the tests, the temperatures were also determined at the same locations as the CO_2 concentrations.

Figures 4 and 5 show the CO_2 and temperatures measured in a test with a 50-kW fire and 32 exhaust inlets located at the 3.5-m (11.4-ft) height. The temperature and CO_2 profiles were used to determine the location of the steady-state smoke interface. Under the specified test condition, the smoke interface was 3 m (9.8 ft) above the floor and approximately 0.5 m (1.6 ft) below the level of the exhaust inlets.

The temperature profile shown in Figure 5 is typical of the test results obtained with the facility. The temperature in the upper hot layer was approximately constant with height, indicating the formation of a stable hot zone. At the smoke interface, the temperature decreased over a transition zone to near ambient conditions. In this case, the transition zone had a depth of approximately 0.5 m (1.6 ft).

The CO_2 concentrations, shown in Figure 4, show the same general trends as those noted for the temperature plots, that is, a stable upper layer in which the CO_2 concentrations were approximately constant. The major difference between the CO_2 and temperature measurements was the gradient in the transition zone. Unlike the temperature results, which varied with height in the transition zone, the CO_2 concentrations typically had a step change at the smoke interface.

The temperature and CO_2 measurements generally indicated the same height for the smoke interface. However, the step change in the CO_2 measurements provided a more accurate estimate of the interface height, and this parameter was used as the primary means of determining its location. The temperature measurements were used as a secondary check. This secondary check was particularly important in the low heat release rate tests in which there was a small increase in CO_2 concentrations (< 0.1% by volume). Such small changes in concentrations were marginal for measurement purposes.

Upper Layer Smoke Temperature

An estimate of the average plume temperature can be determined using the first law of thermodynamics (Klote 1994). Such analysis leads to the following equation for plume temperature:

$$T_p = T_a + \frac{\dot{Q}_c}{\dot{m} C_p} \qquad (6)$$

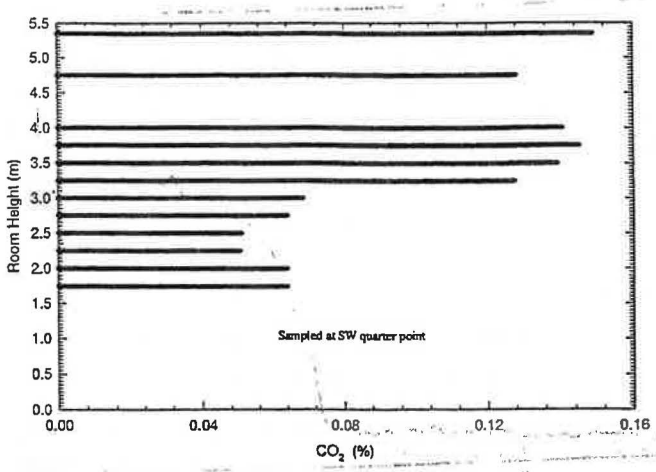

Figure 4 CO_2 concentrations at southwest quarter point for a 50 kW heat release rate.

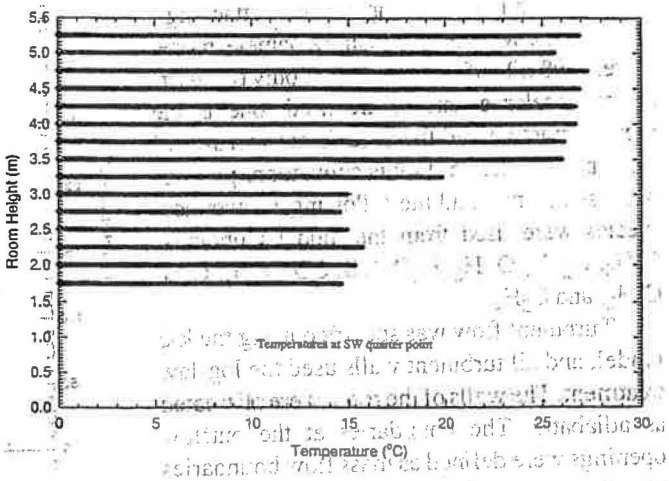

Figure 5 Temperature at southwest quarter point for a 50 kW heat release rate.

where

T_p = average plume temperature at elevation z, °C;
T_a = ambient temperature, °C;
Q_c = convective heat release rate, kW;
$\dot{m}$ = mass flow rate at height z, kg/s; and
C_p = specific heat of plume gases, kJ/kg·°C.

For an upper layer with little heat transfer to the atrium walls and ceiling and small radiative heat transfer from the smoke layer, the upper layer can be thought of as adiabatic or as having negligible heat transfer (Klote 1994). Under such conditions, Equation 6 can be used to estimate the average temperature in the upper layer and the temperature in the exhaust gases.

In order to use Equation 6, an estimate for the smoke production by the fire, including air entrained in the plume, is required. A number of researchers have developed models for turbulent plumes above a fire in building spaces (for example, McCaffrey 1983; Cetegen et al 1982; Heskestad 1984). The work by Heskestad was the basis for the plume mass flow equations used in NFPA 92B (1995) and is used in this paper.

For an axisymmetric plume, the mass flow rate can be approximated using the simple plume equation provided in NFPA 92B (1995). For a steady-state condition, the mass flow rate into the upper layer is given by

$$\dot{m} = C_1 Q_c^{1/3} z^{5/3} + C_2 Q_c \qquad (7)$$

where

Q_c = convective heat release rate, kW;
$\dot{m}$ = mass flow rate at height z, kg/s;
z = clear height above the top of the fuel, m;
C_1 = 0.071; and
C_2 = 0.0018.

For the steady-state tests in the physical model facility, the upper layer interface height determined experimentally was used with Equation 7 to estimate the mass flow rate of hot gases into the upper layer under steady-state conditions. The estimated smoke mass flow rate was used with Equation 6 to estimate the increase in the upper layer temperature.

There was no provision to control the ambient temperature in the test facility. Tests were conducted with ambient temperatures in the range of 5°C to 30°C (41°F to 86°F). A comparison of the average temperature increase in the upper layer measured using similar test configurations indicated that the increase in upper layer temperature did not depend substantially on the ambient conditions.

The calculation of smoke flow rate into the upper layer and the upper layer temperature were carried out using the simple plume method included in the ASMET set of engineering tools (Klote 1994). For these calculations, the convective heat release rate was assumed to be 70% of the measured total heat release rate. A comparison of the increase in upper layer temperature measured experimentally with the model results is shown in Figure 6. The results indicate that the adiabatic temperature

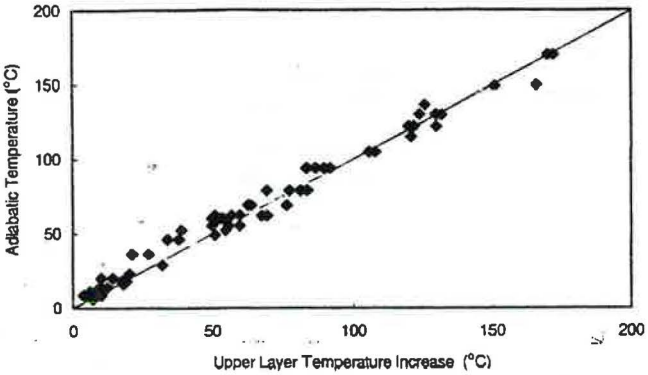

Figure 6 *Correlation of experimental temperature increase with adiabatic temperature increase in upper layer.*

increase tends to be slightly higher than the experimental results. However, considering the wide range of test parameters, there is a good correlation between the measured and estimated temperature increase.

Smoke Exhaust Rate

The principle of conservation of mass for a steady process (Equation 7), which gives the mass flow rate of smoke into the upper layer, also defines the amount of smoke exhausted using the fan system under steady-state conditions. In an ideal smoke management system, the smoke exhaust rate should be equivalent to the rate of smoke production. However, in the physical model tests, one objective was to investigate situations in which the smoke exhaust system was not operating at maximum efficiency. This was accomplished by locating the exhaust inlets at levels near or below the level at which the steady-state smoke interface would normally occur for a specified condition (volumetric exhaust rate and heat release rate). Under these conditions, cold air was entrained with the smoke produced by the fire.

In practice, it was possible to produce situations with a high percentage of the air in the exhaust system (up to 75%) consisting of air entrained from the lower layer. This is illustrated by the comparison of mechanical exhaust rates vs. smoke production shown in Figure 7. For this comparison, the smoke mass production rate was estimated using Equation 7. Using the calculated upper layer temperature and the ideal gas law, the volumetric flow of smoke into the upper layer can be estimated:

$$\dot{V} = \frac{\dot{m}}{\rho_p} \qquad (8)$$

where

$\dot{V}$ = volumetric flow of exhaust gases, m^3/s;
ρ_p = density of exhaust gases, kg/m^3.

The volumetric flow rate determined using Equation 8 is the smoke flow rate into the upper layer at the adiabatic temperature for the upper layer. The procedure, as outlined above, is frequently used to design a mechanical smoke exhaust system with the volumetric flow rate defined by Equation 8 used to

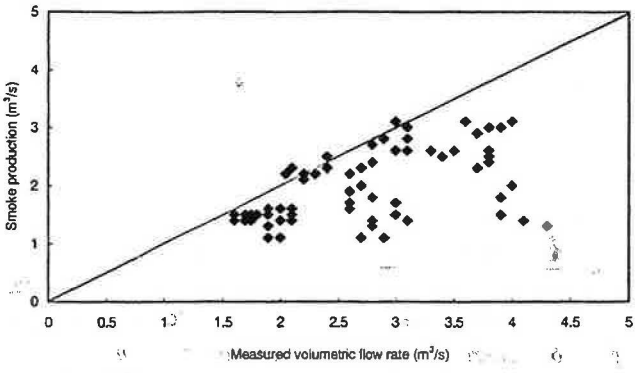

Figure 7 Correlation of smoke production with exhaust rate.

determine the capacity of the mechanical exhaust system. This includes the systems defined in the BOCA (1996) and UBC (ICBO 1994) model codes.

The volumetric flow rate measured in the main exhaust duct was at a considerable distance (> 30 m [98.4 ft]) from the test compartment. As such, there was substantial cooling of the exhaust gases (an approximate 25% to 40% temperature decrease) in the duct before reaching the measurement location. In order to compare the smoke production rate with the measured exhaust rate, both volumetric rates were referenced to ambient conditions (20°C [68°F]).

There are two important factors that can be noted with regard to the correlation results presented in Figure 7.

- For cases in which there was a well-developed smoke layer below the exhaust inlets, the measured exhaust flow rate was comparable to the smoke production rate. These results suggest that, under good operating conditions, the method outlined above for determining the design of an atrium smoke exhaust system under steady-state conditions produces a good estimate for the design of such systems.
- By locating the exhaust inlets at or below the level where the smoke interface would be located with a given set of test conditions (fan capacity and heat release rate), it was possible to produce a range of situations in which the exhaust system entrained a relatively large amount of cold air along with the smoke. Figure 7 indicates that the ratio of mechanical exhaust rate to the smoke production achieved in the test series ranged from 1:1 to 4:1.

CO_2 Concentrations

The CO_2 concentrations measured in the upper layer in the compartment and in the duct can be used to provide further information on the rate of cold air entrainment into the exhaust system. In Figure 8, the ratio of the CO_2 levels measured in the room to the CO_2 concentration measured in the duct is compared to the ratio of the mechanical exhaust rate to the rate of smoke production. For this comparison, the ambient CO_2 concentration was subtracted from the measured concentration.

The general trends indicated in Figure 8 are as follows.

- For an ideal system with the mechanical exhaust rate equivalent to the rate of smoke production, the amount of CO_2 measured in the duct was comparable to that measured in the compartment.
- For those cases with a mechanical exhaust rate higher than the rate of smoke production, there was a decrease in the relative CO_2 levels measured in the exhaust duct, indicating that the smoke was diluted by air entrained from the cold layer.

The maximum dilution indicated by the CO_2 data is approximately 3:1. This is consistent with the smoke exhaust rate and smoke production rate results discussed in the previous section.

Smoke Depth Below Exhaust Inlet

The clear height in the atrium physical model is shown in Figures 9 and 10 for a series of tests with 50-kW and 300-kW heat release rate fires, respectively. Also shown for each test is the height of the exhaust duct inlet and the smoke depth below the exhaust inlet.

Tests 1 through 5 with a 50-kW fire source (Figure 9) were conducted with four exhaust inlets located at various heights with the volumetric flow rate in the main exhaust duct maintained approximately constant. For tests with the inlets at 5.5 and 4.5 m (18 and 14.7 ft), the clear height remained constant at approximately 3.5 m (11.4 ft). However, when the exhaust inlet was located at this level, the clear height formed approximately 0.5 m (1.6 ft) below the exhaust inlet.

Tests 6 through 8 were conducted with 16 exhaust inlets. The volumetric flow rate in the exhaust duct was about 30% higher in these tests. As a result, the exhaust system could maintain a higher clear height, as indicated in test 8. For the tests (tests

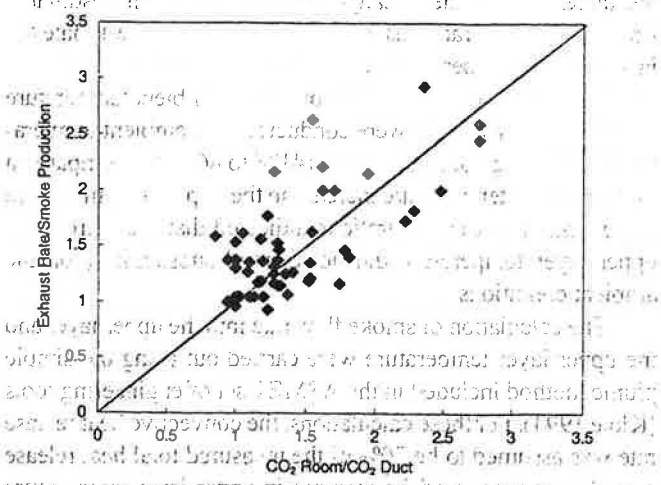

Figure 8 Correlation of CO_2 concentrations with exhaust efficiency.

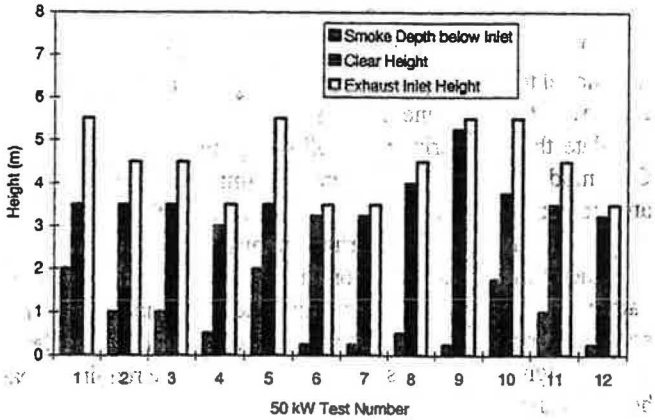

Figure 9 Steady-state smoke layer results for 50 kW heat release test.

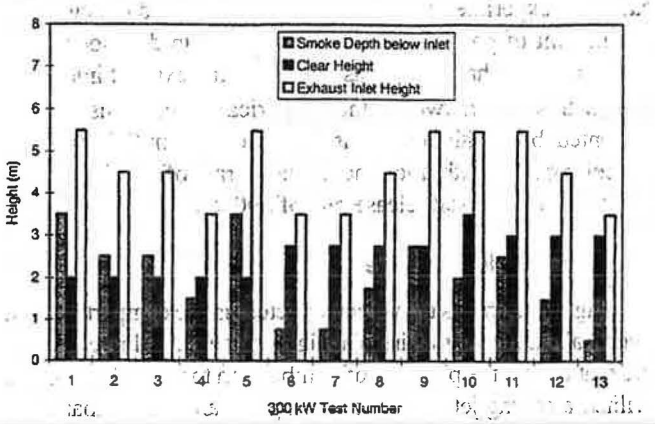

Figure 10 Steady-state smoke layer results for 300 kW heat release rate test.

6 and 7) with the exhaust inlet below the clear height, which could normally be maintained with the experimental exhaust rate, a relatively thin (approximately 0.25 m [0.82 ft] deep) smoke layer formed below the exhaust inlet height.

For tests 9 through 12, with 32 exhaust inlets, higher clear heights could be maintained in the facility. As in the tests with the 16 exhaust inlets, the smoke depth below the exhaust inlet height was minimal for the case with the inlets located below the height at which the smoke layer interface would normally be maintained with the experimental exhaust rate.

For the 300-kW fire source, tests 1 through 5 were with 4 exhaust inlets, tests 6 through 9 were with 16 exhaust inlets, and Tests 10 through 13 were with 32 exhaust inlets. The clear heights were approximately constant for each group of tests. The clear height was primarily dependent on the volumetric flow rate in the exhaust system. Tests with a 0.5 to 0.75 m (1.6 ft to 2.4 ft) smoke layer depth below the exhaust inlet did not change the clear height, indicating that the mechanical exhaust system was still efficient for these cases. That is, the mechanical exhaust rate was equivalent to the rate of smoke production.

These results are consistent with the general trends observed in the physical model tests. These trends are as follows.

- If the exhaust inlets were located well above the clear height, the location of the exhaust inlets did not impact the effectiveness of the mechanical exhaust system. The location of the smoke interface was dependent on the capacity of the exhaust system and the plume dynamics. As discussed previously, the simple plume equations provided a good estimate of the smoke flow into the upper layer.
- If the exhaust inlets were located at or below the height for which the mechanical system had sufficient capacity to maintain a clear height, the smoke layer formed below the exhaust inlets. The depth of this smoke layer was typically less than 1 m (3.2 ft) and, in some cases, was limited to 0.25 m (0.82 ft).

The latter case is the situation under investigation in this project. That is, if an atrium smoke management system is required with the exhaust inlets close to the design clear height, what is the potential impact on the mechanical exhaust effectiveness? The preliminary results obtained in this project indicate that, in this case, a stable smoke interface will form some distance below the height of the exhaust inlets. The exhaust gases will include both entrained air from the lower cold layer and the smoke produced by the fire.

Further analysis of the small-scale test results as well as the results of the full-scale tests will be required to determine the parameters that affect the depth of the smoke layer below the exhaust inlets and the scaling of this depth to full scale. In the following section, one model for cold air entrainment into a venting system is discussed.

Plugholing

Cold air entrainment into a smoke-venting system is addressed by Hinckley (1995). Based on investigations with gravity venting systems, it was determined that the onset of the plugholing phenomenon depends on a Froude number, Fe:

$$Fe = V_v/[(g\theta/T_o)^{1/2} d_e^{5/2}] \qquad (9)$$

where

V_v = volume rate of flow, m^3/s;
d_e = depth of hot gases below the exhaust inlet, m;
θ = temperature above ambient, K;
T_o = ambient temperature, K; and
g = acceleration due to gravity, m/s^2.

Work on vents indicates that a Froude number of 1.5 is applicable for vents near the center of a smoke reservoir and 1.1 is applicable for vents near the sides (Morgan and Gardiner 1990).

Hinckley (1995) defines Equation 9 in terms of the smoke depth. However, the equation was developed assuming the smoke vent systems were located in the ceiling. In the following analysis, it is assumed that the smoke depth in Equation 9 represents the distance between the exhaust inlet and the clear height.

Plots for maximum volumetric flow rate vs. smoke depth are shown in Figure 11 for smoke temperatures of 10°C (50°F), 50°C (122°F), 100°C (212°F), 150°C (302°F), and 200°C (392°F) above ambient using a Froude number of 1.1. The temperature increases are representative of those measured in the physical model tests.

For the physical model tests, the volumetric flow rate per exhaust inlet was in the range of 0.1 to 0.5 m^3/s, depending on the number of exhaust inlets that were open and the operating speed of the fan. For this volumetric flow range, Figure 9 indicates that problems with air entrainment would occur for smoke depths between 0.5 and 1.0 m (1.6 and 3.2 ft) for small increases (10°C and 20°C [50°F and 68°F]) in upper layer temperature, such as those produced by the 50-kW heat release rate fires.

As discussed in the previous section, relatively thin smoke layers (0.25 to 0.5 m [0.82 to 1.6 ft]) were measured below the exhaust inlet in some situations with the 50-kW heat release rate fires. However, in these cases, the exhaust rate was much greater than the smoke production rate (> 2:1), indicating air entrainment from the cold layer along with the smoke produced by the fire. For those cases in which the smoke depth below the exhaust inlets was greater than 1 m (3.2 ft), the exhaust rate was approximately equivalent to the smoke production rate.

For the 300-kW tests discussed in the previous section, the increase in temperature in the upper layer ranges from approximately 50°C (122°F) to 120°C (248°F), depending on the clear height produced. The minimum smoke depth below the exhaust inlets produced in the tests was 0.5 to 0.75 m (1.6 to 2.4 ft). For the range of volumetric flow rates considered in these tests, the exhaust rates were below the limit for the onset of entrainment of cold air for these smoke depths. This is consistent with the results for the tests shown in Figure 10. In all cases, the exhaust rate was approximately equivalent to the smoke production rate (within ±20%).

The preliminary analysis in this section indicates that the results with the physical model tests are consistent with the model for the onset of cold air entrainment provided by Hinckley (1995). The model will be used as one basis for developing design guides for the onset of cold air entrainment in a smoke management system.

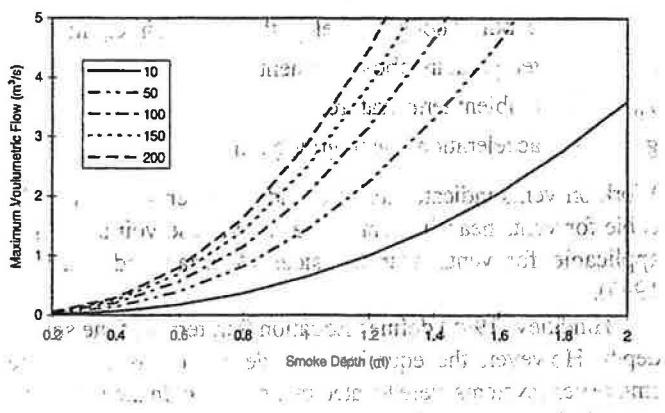

Figure 11 Maximum volumetric flow versus smoke depth

CFD MODEL RESULTS

The CFD model was used to simulate a number of the physical model tests. The primary purpose of the numerical simulations was to determine whether the model could accurately simulate these experiments. Following model validation, the CFD model will be used to carry out simulations for large-scale atria to determine whether those experimental findings regarding the effectiveness of the atrium exhaust system that are based on scale-modeling are valid for large-scale applications. This is particularly important in determining the minimum depth of the smoke layer below an exhaust inlet, which should be considered in the design of an exhaust system to provide the required clear height in an atrium.

The heat release rate and smoke exhaust rate, used for the numerical simulations, were obtained from the experimental data. The experimental heat release rate was used to determine the amount of propane that was consumed in the model. The experimental exhaust rate was defined at the exhaust inlets.

In this paper, two of the numerical simulations will be presented, both with the exhaust inlet located 1 m (3.2 ft) below the ceiling: one with a low heat release rate of 50 kW and the other with a high heat release rate of 200 kW.

Low Heat Release Rate

Figure 12 shows the velocity vectors in the compartment on a vertical plane over the fire. The figure shows the plume over the fire that carries the products of combustion to the ceiling. At the ceiling, a ceiling jet develops moving toward the compartment walls. A flow reversal occurs at the wall, causing the hot gases to start moving toward the center of the room. This flow reversal is due to the cold air that enters the room at the floor level, as seen by the vectors at the left bottom corner. The incoming fresh air moves upward and almost reaches the room mid-height before it

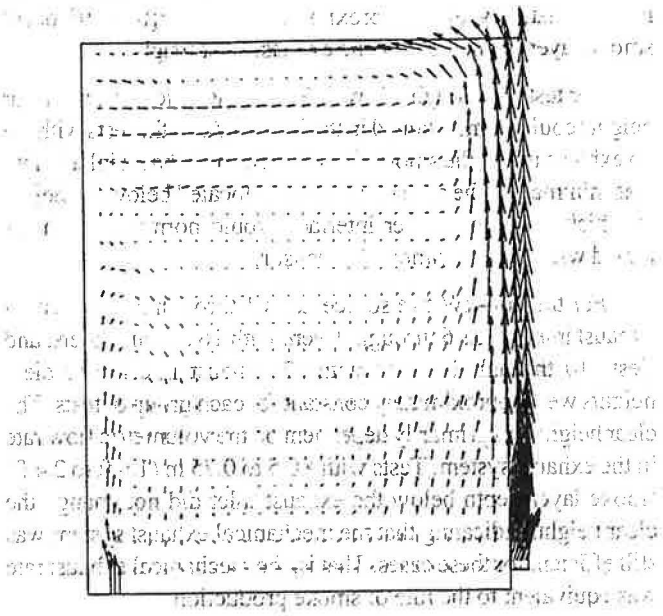

Figure 12 Velocity vectors for 50 kW fire (maximum velocity 3 m/s)

loses its momentum and starts to descend. The velocity of the incoming air at the entry point is about 1 m/s (3.2 ft/s), while the maximum velocity in the fire plume is about 3 m/s (9.8 ft/s).

Figure 13 shows the temperature contours in the same plane as the velocity vectors in Figure 12. For the visualization of the hot layer, the maximum temperature shown was limited to 560°C (1040°F). The figure shows small temperature rises outside the plume. Isothermal line 2 represents a temperature of only 37.5°C (99.5°F) and isothermal line 3 represents a temperature of 65°C (149°F). The temperature difference between isothermal lines is 27.5°C (49.5°F).

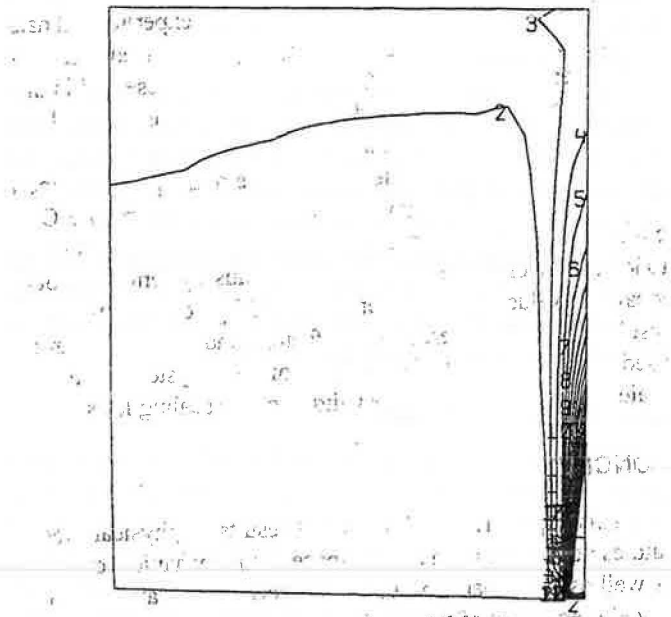

Figure 13 Temperature contours for 50 kW fire, contour 2 at 37.5°C and temperature difference between contours 27.5°C.

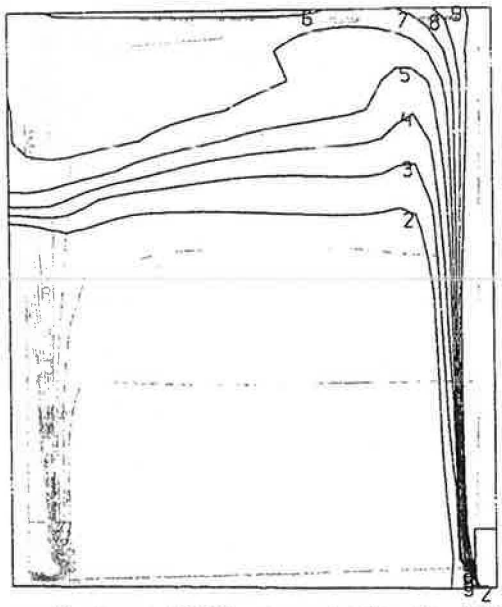

Figure 14 Contours of CO_2 concentration for 50 kW fire, contour 2 at 0.00075 and difference between contours 0.00025.

Figure 14 shows isolines for CO_2 concentrations in the enclosure. Isoline 2 represents a concentration of 0.00075. The difference between isolines is 0.00025. The maximum CO_2 concentration outside the fire plume is 0.0025, represented by isoline 9.

Figure 15 shows a comparison of the temperature profiles at the room quarter point between experimental and numerical temperatures. The model seems to overpredict the temperature near the ceiling and shows a temperature gradient within the hot layer, while the experimental data indicate that the temperature in the hot layer is uniform. The same trend is seen in Figure 16, which shows a comparison between the experimental and numerical CO_2 profiles.

Despite the difference in the local CO_2 and temperature values between the model predictions and the experimental data, there is a good agreement between the experimental and numerical clear height in the compartment, as well as the average hot layer temperature and CO_2 concentrations. The experimental average hot layer temperature was found to be 41°C (105.8°F)

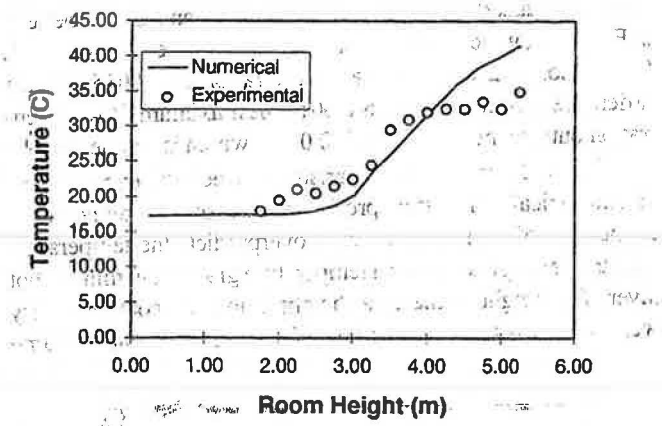

Figure 15 Comparison of experimental and predicted temperature profiles for 50 kW fire at room quarter points.

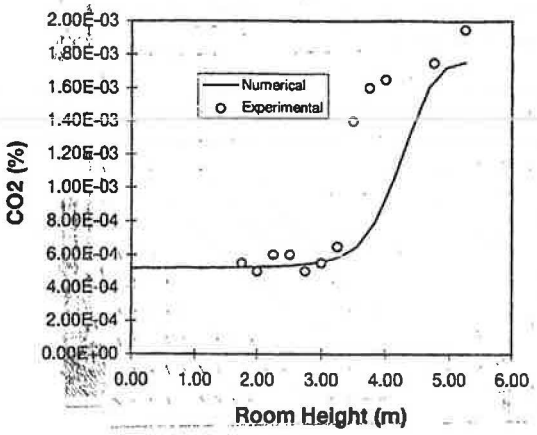

***Figure 16** Comparison of experimental and predicted CO_2 concentration profiles for 50 kW fire at room quarter point.*

and the predicted temperature was found to be 38°C (100.4°F), while the average predicted CO_2 concentration was 0.0019 and the experimental concentration was 0.0017.

High Heat Release Rate

The simulation of the 200-kW heat release rate fire shows the same trends as the simulation for the 50-kW case. The velocity vectors over the vertical plane passing through the fire, shown in Figure 17, present a flow structure similar to that seen in Figure 12. In this case, however, the stream of incoming fresh air only reaches up to about the quarter height of the room and then reverses direction, moving downward. A stronger recirculating flow is established within the hot layer, moving the hot gases from the fire plume toward the enclosure walls and then diffusing them into the hot layer.

The isothermal lines shown in Figure 18 indicate that temperatures of more than 60°C (140°F) (isothermal line 2) exist in the room at a level of about 2 m (6.5 ft) from the floor. The bulk of the hot layer has temperatures ranging from 110°C (230°F) (isothermal line 3) to 160°C (320°F) (isothermal line 4). The temperature difference between isolines in this figure is 50°C (90°F).

The reduced clear height of this simulation can also be seen in Figure 19, which depicts isolines of CO_2 concentration. In this figure, isoline 2 represents a concentration of 0.0015 and the difference between isolines is 0.001. The maximum CO_2 concentration outside the fire plume is 0.0095, which is isoline 10.

Figure 20 shows a comparison between the experimental and numerical temperature profiles at the room quarter point. As in the case of 50 kW, the model overpredicts the temperature near the ceiling and shows a temperature gradient within the hot layer. The height of the clear height, however, compares very well. The CO_2 profiles, shown in Figure 21, present the same trends as the low heat release rate case. The experimental data have a uniform CO_2 concentration in the hot layer, while the predicted CO_2 concentrations have a continuous increase from the interface to the ceiling.

The estimated clear height from the model results is at about 3.6 m (11.8 ft) and the experimental clear height is at 3.5 m (11.4 ft). The predicted average CO_2 concentration in the hot layer is 0.0060 and the experimental concentration is 0.0066. The predicted average temperature is 124°C (255.2°F) while the experimental temperature is 125°C (257°F).

The results of the comparisons between experimental data and model predictions indicate that, while localized comparisons of temperatures and CO_2 concentrations presented in this paper do not show very good agreement, the averaged values, such as hot layer temperature, CO_2 concentration, and clear height, agree very well. Due to the nature of the problem, good agreement of localized comparisons of temperature and CO_2 concentrations is not expected. As the objective of this study is to look at the effectiveness of atrium exhaust systems and not at localized values of temperature and CO_2 concentration, the results can be considered as satisfactory and the model can be used to determine the effectiveness of these systems in a full-scale atrium to determine the validity of the scaling laws.

CONCLUSIONS

This paper presented the initial results of physical model studies performed in an atrium space with mechanical exhaust, as well as a comparison between experimental data and CFD model predictions of the conditions in the atrium space. It also investigates the effect of fire size and opening location on the conditions in the atrium.

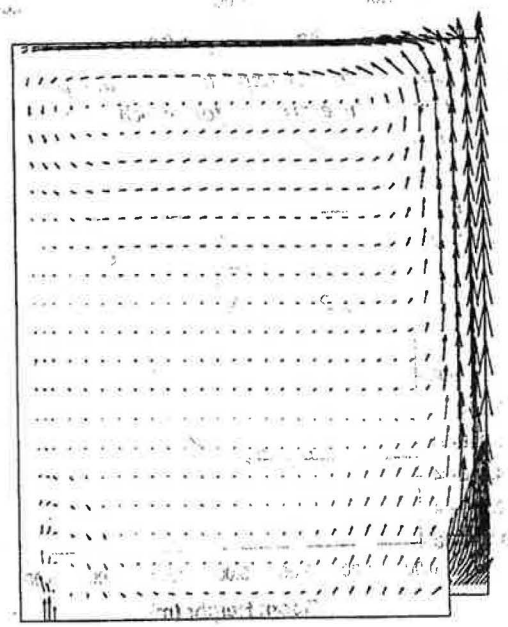

Figure 17 Velocity vectors for 200 kW fire (maximum velocity 4.2 m/s).

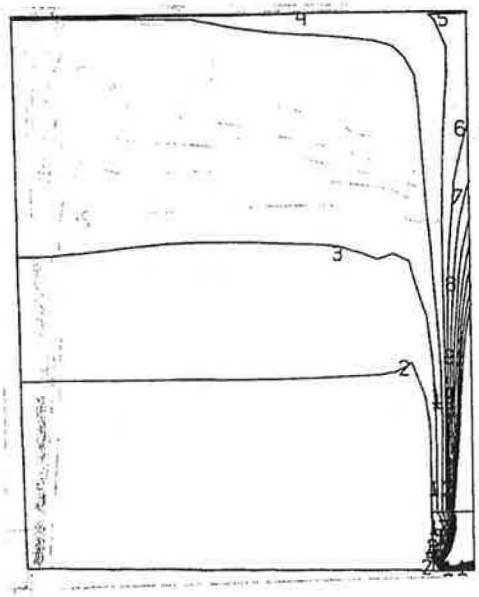

Figure 18 Temperature contours for 200 kW fire, contour 2 at 60°C and temperature difference between contours 50°C.

The initial results indicate that, for the atrium studied, the correlations in NFPA 92B (1995) used for the design of exhaust systems are valid, as the results of these equations compare well with the experimental findings. The results also demonstrate that, when the exhaust systems operate near or just below their design capacity, they are effective in extracting gases from the hot layer without drawing in air from the lower layer. As expected, when the systems operate well above the required flow rates, fresh air from the lower layer enters the system. This, however, does not make the system ineffective, as the level of the hot layer remains at an acceptable height.

Comparisons of experimental data with CFD model predictions indicate that, while a one-to-one comparison of temperature and CO_2 does not give very good results overall, the CFD model was able to predict the level of the hot layer as well as the average conditions in this layer.

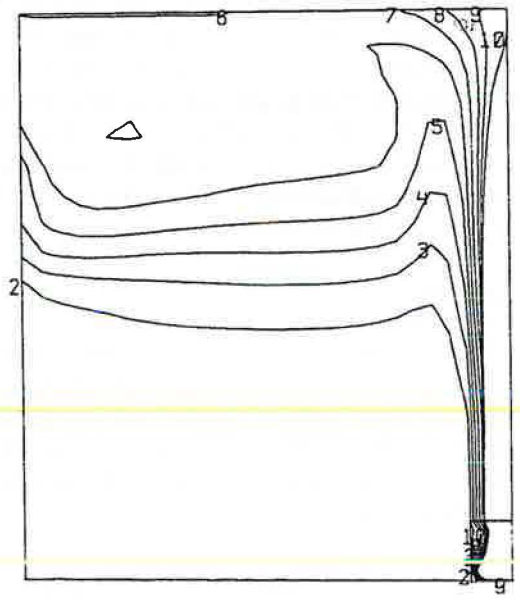

Figure 19 *Contours of CO_2 concentration for 200 kW fire, contour 2 at 0.0015 and difference between contours 0.001.*

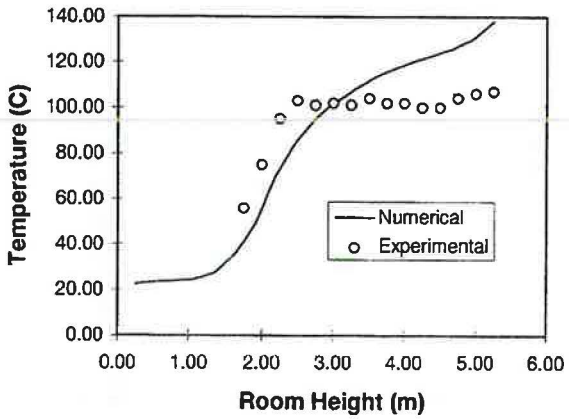

Figure 20 *Comparison of experimental and predicted temperature profiles for 200 kW fire at room quarter points.*

ACKNOWLEDGMENTS

This paper is based on a research project conducted at the National Research Council of Canada in partnership with the American Society of Heating, Refrigerating and Air-Conditioning Engineers, Inc., which provided both financial support and project feedback through its Technical Committee 5.6. The experiments were conducted by Bruce Taber and Cam McCartney and the CFD runs were done by Shu Cao.

REFERENCES

ASC. 1994. *TASCflow user documentation*, version 2.3. Waterloo, Ont.: Advanced Scientific Computing Ltd.

BOCA. 1996. The BOCA national building code. Country Club Hills, Ill.: Building Officials and Code Administrators International Inc.

Cetegen, B.M., E.E. Zukowski, and T. Kubota. 1982. Entrainment and flame geometry of fire plumes, Ph.D. thesis of Cetegen, California Institute of Technology, Pasadena.

Degenkolb, J.G. 1975. Fire safety for atrium type buildings. *Building Standards* 44: 16-18.

Degenkolb, J.G. 1983. Atriums. *Building Standards* 52: 7-14.

Hansell, G.O., and H.P. Morgan. 1994. *Design approaches for smoke control in atrium buildings*. BR-258. Garston, U.K.: Building Research Establishment.

Heskestad, G. 1984. Engineering relations for fire plumes. *Fire Safety Journal* 7: 25-32.

Hinckley, P.L. 1995. Smoke and heat venting. In *SFPE Handbook of Fire Protection Engineering*, pp. 3-160 to 3-173. Quincy, Mass.: National Fire Protection Association.

ICBO. 1994. *The uniform building code*. Whittier, Calif.: International Conference of Building Officials.

Klote, J.K. 1994. Method of predicting smoke movement in atria with application to smoke management. NISTIR

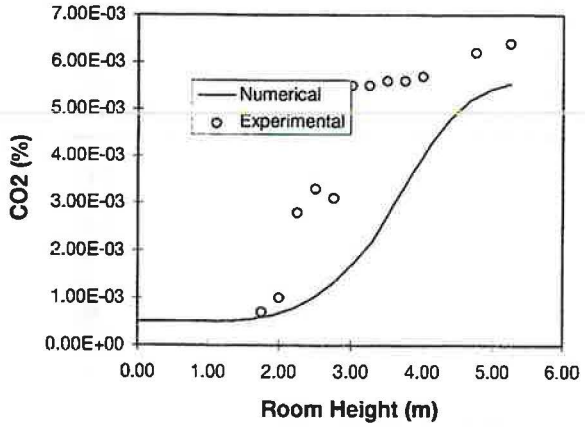

Figure 21 *Comparison of experimental and predicted CO_2 concentration profiles for 200 kW fire at room quarter point.*

5516. Gaithersburg, Md.: National Institute of Standards and Technology.

Klote, J.K., and J.A. Milke. 1992. *Design of smoke management systems*. Atlanta: American Society of Heating, Refrigerating and Air-Conditioning Engineers, Inc.

McCaffrey, B.J. 1983. Momentum implications for buoyant diffusion flames. *Combustion and Flame* 52: 149-167.

Morgan, H.P., and J.P. Gardiner. 1990. *Design principles for smoke ventilation in enclosed shopping centres*. BR 186. Garston, U.K.: Building Research Establishment.

NBCC. 1995. National building code of Canada. Ottawa, Canada: National Research Council Canada.

NFPA. 1995. *NFPA 92B, Guide for smoke management systems in malls, atria, and large areas*. Quincy, Mass.: National Fire Protection Association.

NFPA. 1996. *NFPA 13, Standard for the installation of sprinkler systems*. Quincy, Mass.: National Fire Protection Association.

Peters, N. 1984. Laminar diffusion flamelet models in non-premixed turbulent combustion. *Progress in Energy and Combustion Science* 10(3): 319-339.

Peters, N. 1986. Laminar flamelet concepts in turbulent combustion. *21st Symposium (International) on Combustion/The Combustion Institute*, pp. 1231-1250.

Spratt, D., and A.J.M. Heselden. 1974. Efficient extraction of smoke from a thin layer under a ceiling. Fire Research Note No. 1001. London: U.K. Joint Fire Research Organisation.

Tamura, G.T. 1995. *Smoke movement and control in high-rise buildings*. Quincy, Mass.: National Fire Protection Association.

Yamana, T., and T. Tanaka. 1985. Smoke control in large spaces. Part 2: Smoke control experiments in a large scale space. *Fire Science* 5: 41-54.